VIII. PHYSICAL ELECTRONICS AND SURFACE PHYSICS

A. Surface Physics*

Academic and Research Staff

Prof. R. E. Stickney
Dr. M. L. Shaw

Graduate Students

J. W. Gadzuk
R. M. Logan
D. S. Shupe

1. SINGLE PHONON ACCOMMODATION COEFFICIENTS

Introduction

It is our present purpose to report some recent improvements in quantum-mechanical accommodation theory.[1-5] This study will be reported in detail later.

The essence of the existing theories may be described as follows. An inert gas atom such as helium, described by an initial wave function $\phi'(r)$, undergoes a collision with a bound surface atom of a lattice described by an assumed harmonic oscillator wave function $\psi_n(u)$. A single quantum of energy is transferred in the process. The final state of the atom is taken to be $\phi(r)$, and that of the metal atom $\psi_{n\pm1}(u)$. The matrix element for the process is given by

$$B_{n,n-1} = \iint d^3r\, d^3u\, \phi^*(\bar{r})\, \psi_n^*(\bar{u}) \left[V_a(\bar{r}-\bar{u}) - V_a(\bar{r}) \right] \psi_{n-1}(\bar{u})\, \phi'(r), \tag{1}$$

with

$$V(\bar{r}-\bar{u}) = V(\bar{r}) - \bar{u} \cdot \nabla V(\bar{r}) + \frac{1}{2} \bar{u}_i \bar{u}_j \cdot \nabla^2 V(\bar{r}) - \ldots . \tag{2}$$

The accommodation coefficient is given by an expression of the form

$$\alpha_o = \gamma |B_{n,n-1}|^2 \tag{3}$$

where γ contains statistical factors, density of states, constants, and so forth. The point is that α, the AC, is proportional to the square of the matrix element. These results are not necessarily in agreement with experimentally determined AC.

*This work was supported by the Joint Services Electronics Programs (U.S. Army, U.S. Navy, and U.S. Air Force) under Contract DA 36-039-AMC-03200(E).

Theory

There should be a great similarity between the lattice theories of neutron scattering, Mössbauer effect, and inert-gas scattering. In all cases the lattice is perturbed by some external probe – the neutron, recoiling nucleus or incident gas atom – and the number of phonons is the lattice displacement field changes by some small number, usually zero or one. Guided by the existing neutron[6] and Mössbauer effect[7] theories, we proceed in an extremely cavalier fashion.

The lattice is normal-mode analyzed and second-quantized in the manner of Pines.[8] The lattice state is described in the occupation number representation in which the state vectors are eigenfunctions of the phonon number operator. With the use of Boson creation and annihilation operators, the necessary mathematical aspects of the Bosen field may be summarized:

$$H_L|n\rangle = \sum_{q,j} \hbar\omega_{q,j}\left(a^\dagger_{q,j}a_{q,j}+\tfrac{1}{2}\right)|n\rangle = \sum_{q,j} \hbar\omega_{q,j}\left(n_{q,j}+\tfrac{1}{2}\right)|n\rangle \quad \left(\begin{matrix}\text{Eigenfunction}\\ \text{Equation}\end{matrix}\right) \tag{4a}$$

$$\left[a^\dagger_{q,j}, a_{q'j'}\right] = \delta_{q,q'}\delta_{j,j} \quad \text{(Commutation)} \tag{4b}$$

$$\left[a^\dagger_{q,j}, a^\dagger_{q'j'}\right] = \left[a_{qj}, a_{q'j'}\right] = 0$$

$$\langle n_q+1|a^\dagger_q|n_q\rangle = \sqrt{n_q+1} \quad \text{(Orthonormality)} \tag{4c}$$

$$\langle n_q-1|a_q|n_q\rangle = \sqrt{n_q}$$

$$\langle m|n\rangle = \delta_{m,n}$$

$$n_{q,j} = \left[e^{\hbar\omega_{q,j}/kT}-1\right]^{-1} \quad \left(\begin{matrix}\text{Thermal}\\ \text{Equilibrium}\end{matrix}\right) \tag{4d}$$

It is assumed that the displacement of surface atoms is adequately described in terms of bulk-mode displacements. The surface atom undergoing collision is assumed to be at the origin of the coordinate system. Thus the usual expression for the atom displacement is

$$\bar{u}_\ell = \sum_{q,j}\left(\frac{\hbar}{2MN\omega_{q,j}}\right)^{1/2}\left(\hat{e}_{q,j}a_{q,j}+\hat{e}_{-q,j}a^\dagger_{q,j}\right). \tag{5}$$

By following the lines of Lipkin,[9] it can be shown that for small displacements, the

interaction of Eq. 2 can be expressed as

$$V_a(\bar{r}-\bar{u}) - V_a(\bar{r}) \simeq e^{-\bar{a}\cdot\bar{u}_\ell} \frac{1}{|a|} \nabla V_a(\bar{r}), \tag{6}$$

where a is a parameter controlling the range of interaction. This result, which will be more rigorously derived in a forthcoming paper, is independent of the functional form of the interaction.

By having the displacement-field operator in an exponential, we have recourse to some field theoretic results derived by Glauber.[10] His result states that the operator deriving from $e^{-\bar{a}\cdot\bar{u}}$, which induces an n phonon transition is given by

$$\left\langle e^{-a\cdot u_\ell} \right\rangle_T^{(n)} = \frac{(-\bar{a}\cdot\bar{u}_\ell)^n}{n!} e^{\frac{1}{2}\left\langle (a\cdot u_\ell)^2 \right\rangle_T}, \tag{7}$$

where the expectation value of the square of the $\bar{a}\cdot\bar{u}_\ell$ operator is taken with respect to the thermally excited equilibrium state given by Eq. 4d. In single phonon transitions, this operator takes into consideration such single-phonon processes in the interaction expansion of Eq. 2 as occur from operators of the form $a_q^\dagger, a_{q'}, a_{q'}^\dagger)$, in which a virtual phonon in the q'^{th} mode is emitted and reabsorbed before the real phonon in the q^{th} mode is emitted. Processes of this sort give rise to the Debye-Waller factor in neutron and Mössbauer theory, and also give rise to a pseudo Debye-Waller factor in the atom-scattering phenomena.

Combining Eqs. 1, 4, 6, and 7 allows the new single-phonon matrix element to be written

$$B'_{n,n-1} = \frac{a}{|a|} \cdot \langle n|u|n-1\rangle \; e^{\frac{1}{2}\left\langle (a\cdot u)^2 \right\rangle_T} \int d^3r \, \phi^*(\bar{r}) \nabla V_a(\bar{r}) \, \phi'(\bar{r}). \tag{8}$$

Since

$$\frac{a}{|a|} \cdot \langle n|u|n-1\rangle = \left(\frac{\hbar n}{2MN\omega}\right)^{1/2}$$

by virtue of Eqs. 4 and 5, it is equivalent to the harmonic oscillator matrix element of Eq. 1. Furthermore, since the atomic matrix element in Eq. 8 is also equivalent to that in Eq. 1, the new matrix element becomes

$$B'_{n,m} = e^{\frac{1}{2}\left\langle (a\cdot u)^2 \right\rangle_T} B_{n,m}$$

and consequently

$$\alpha_n = e^{\left\langle (a \cdot u)^2 \right\rangle_T} \alpha_o. \tag{9}$$

Thus the new AC is simply the existing single-phonon AC multiplied by the pseudo Debye-Waller factor. It is a standard matter to evaluate the thermal mean-square displacement term in the exponent.[8] It can readily be shown that

$$\left\langle (\bar{a} \cdot \bar{u})^2 \right\rangle_T = \frac{\hbar^2 a^2}{mk\theta_D} \left[\frac{1}{4} + \left(\frac{T}{\theta_D} \right)^2 \int_0^{\theta_D/T} \frac{x\, dx}{e^x - 1} \right] \tag{10}$$

with $x = \hbar\omega/kT$. Equation 10 is exactly evaluated in low- and high-temperature limits as

$$\lim_{T \to 0} \left\langle (a \cdot u)^2 \right\rangle_T = \frac{\hbar^2 a^2}{mk\theta_D} \left[\frac{1}{4} + \frac{H^2}{6} \left(\frac{T}{\theta_D} \right)^2 \right]$$

and

$$\lim_{T \to \infty} \left\langle (\bar{a} \cdot \bar{u})^2 \right\rangle_T = \frac{\hbar^2 a^2}{mk\theta_D} \left(\frac{T}{\theta_D} \right). \tag{11}$$

Results

Theoretical AC may be obtained by using Eq. 10 or 11 in Eq. 9 if values for α_o are known. Gilbey[4] gives numerical values of α_o vs temperature for helium. In most

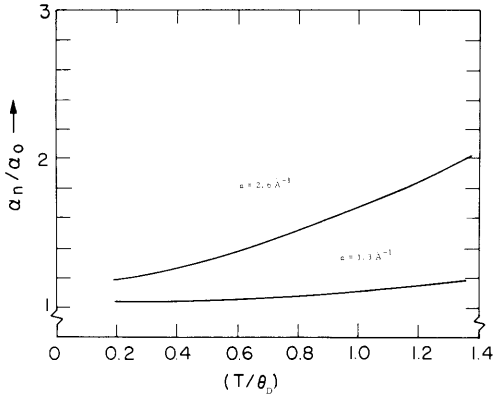

Fig. VIII-1.

Pseudo Debye-Waller correction factor for existing single quantum-accommodation-coefficient theories.

theories, a Morse or exponential repulsive potential describes the interaction. The value of the parameter z in Eq. 6 is closely related to the range parameter in the Morse potential. Since the repulsive portion of the Morse potential varies as $e^{-2a_1 r}$, we take $a_1 \leq a \leq 2a_1$. For the Ne-W system, $a_1 = 1.3$ Å^{-1}. We take $\theta_D = 300°$K for W.

With these numbers, the quantity α_n/α_o vs temperature is drawn in Fig. VIII-1, with a treated parametrically for the temperature range less than the Debye temperature, the region in which the simple quantum-mechanical model is valid. It is seen that a non-trivial correction to the original AC results. In Fig. VIII-2 three AC are drawn: the

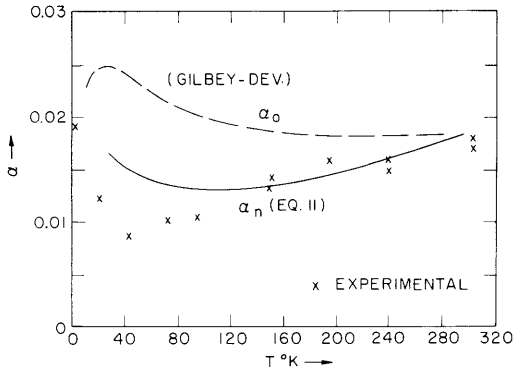

Fig. VIII-2.

Experimental and old and new theoretical accommodation coefficients as a function of temperature for He-W.

uncorrected α_o, the new theoretical α_n given by Eqs. 9 and 11, and experimentally determined AC.[11] All α have been adjusted so as to coincide at T = 300°K. This amounts to multiplying α_o or α_n by a constant that shifts the axis but not the shape of the curve. Clearly, the new AC appears to be in better agreement with experiment than the previous quantum-mechanical expressions. Both the new expression and the data approach a high-temperature limit from below the limit, whereas the old theory approaches the same limit from above. It seems quite reasonable to say that if single-phonon AC are meaningful, then the existing theories should be modified by a pseudo Debye-Waller factor in order that there may be some quantitative agreement.

A more detailed treatment of this theory, together with an adequate discussion of the meaning and significance of these results, is forthcoming.

J. W. Gadzuk

References

1. J. M. Jackson, Proc. Camb. Phil. Soc. 28, 136 (1932).
2. A. F. Devonshire, Proc. Roy. Soc. (London) A158, 269 (1937).
3. J. E. Lennard-Jones and C. Strachen, Proc. Roy. Soc. (London) A150, 442 (1935).
4. D. M. Gilbey, J. Phys. Chem. Solids 23, 1453 (1962).
5. R. T. Allen and P. Feuer, J. Chem. Phys. 40, 2810 (1964).
6. L. S. Kothari and K. S. Sinwi, Solid State Phys. 8, 109 (1954).
7. H. Frauenfelder, The Mössbauer Effect (W. D. Benjamin, Inc., New York, 1963).
8. D. Pines, Elementary Excitations in Solids (W. D. Benjamin, Inc., New York, 1964), Chap. 2.

9. H. J. Lipkin, Ann. Phys. (N. Y.) 9, 332 (1960).

10. R. J. Glauber, Phys. Rev. 84, 395 (1951); 98, 1692 (1955).

11. L. B. Thomas, "Determination of the Thermal Accommodation Coefficient and Research on the Conduction of Heat by Eilute Gases from Solid Surfaces and Its Uses as an indicator of Surface Condition," Final Report of work done under U.S. Army Contracts DA-23-072-ORD--388 and DA-23-072-ORD-990 at the University of Missouri, 1958.

VIII. PHYSICAL ELECTRONICS AND SURFACE PHYSICS

B. Surface Properties of Thermionic Electrodes*

Academic and Research Staff

Prof. R. E. Stickney
J. G. Bergman

Graduate Students

W. Engelmaier
D. L. Fehrs

1. THERMIONIC CHARACTERISTICS OF A SINGLE-CRYSTAL TUNGSTEN FILAMENT EXPOSED TO OXYGEN

Introduction

More than forty years ago, Langmuir and Kingdon[1] observed that the thermionic emission from a cesiated tungsten filament could be increased markedly by adsorbing O_2 upon the filament. Although this problem has received very little attention in subsequent years, it is now being reconsidered because of its possible importance to thermionic energy conversion.[2] In the past five years the number of investigations of the effects of electronegative gases (such as O_2 and F_2) on the thermionic properties of cesiated refractory metals has increased.[3]

The present experiment is designed to investigate the effect of O_2 on the thermionic emission from a single-crystal tungsten filament. Our specific objective is to determine the dependence of the work functions of different crystallographic directions on O_2 pressure and filament temperature.

Descriptions of the experimental apparatus and the preliminary data have been reported in Quarterly Progress Report No. 79, pages 156-166. Hence, we shall concentrate here in the results that were obtained after improving the method of introducing O_2 into the vacuum system. The diffusion-type leak used previously has been replaced by a motor-driven Granville-Phillips valve connected to a one-liter flask of research grade O_2.

Experimental Results

The results shown in Fig. VIII-3 were obtained by increasing the O_2 pressures in small steps while holding the filament at various temperatures. The effective work function, ϕ_E, is computed from the following form of the Richardson equation,

*This work was supported by the National Aeronautics and Space Administration (Grant NGR-22-009-091).

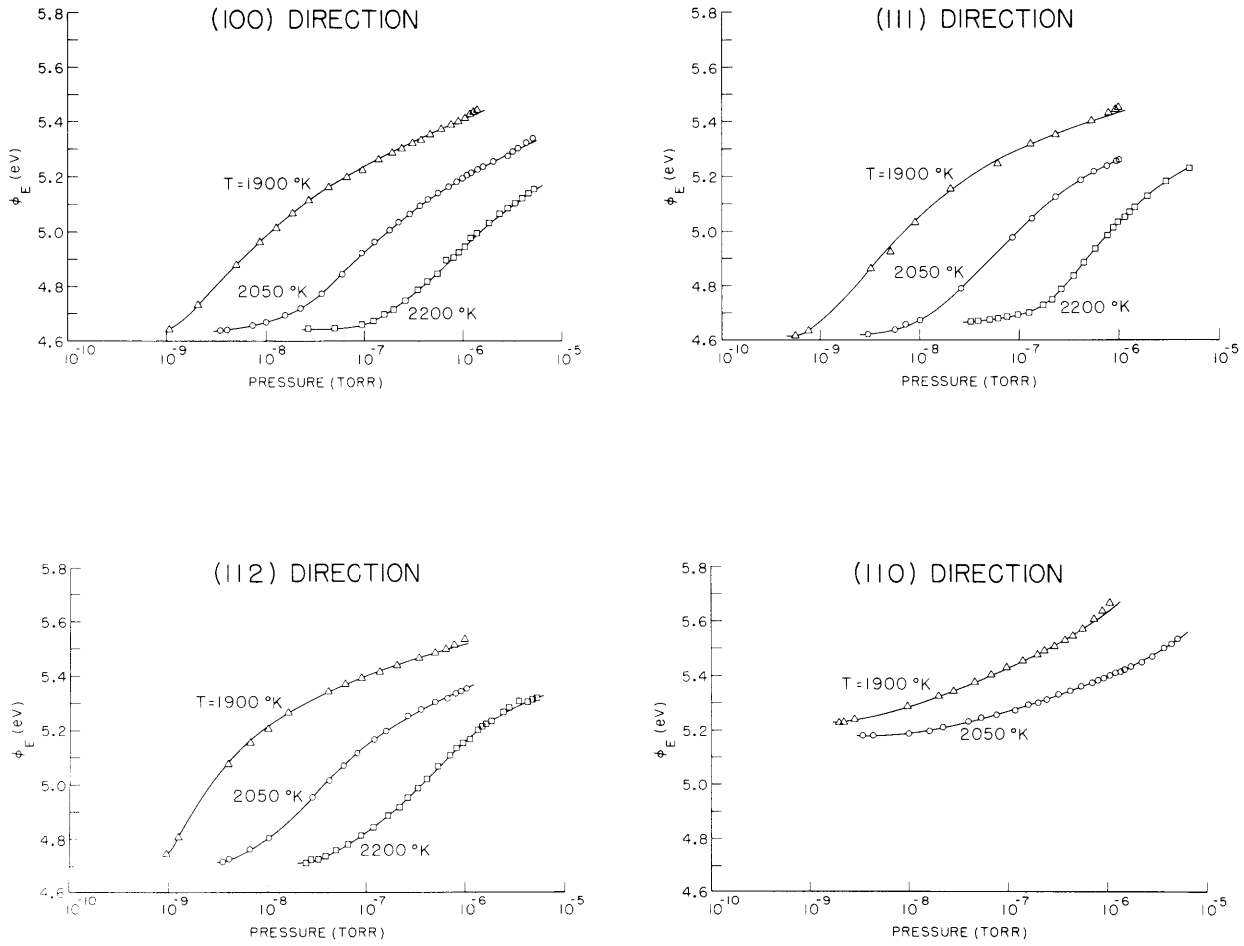

Fig. VIII-3. Effective work functions of the (100), (111), (112), and (110) crystallographic directions as a function of O_2 pressure and filament temperature.

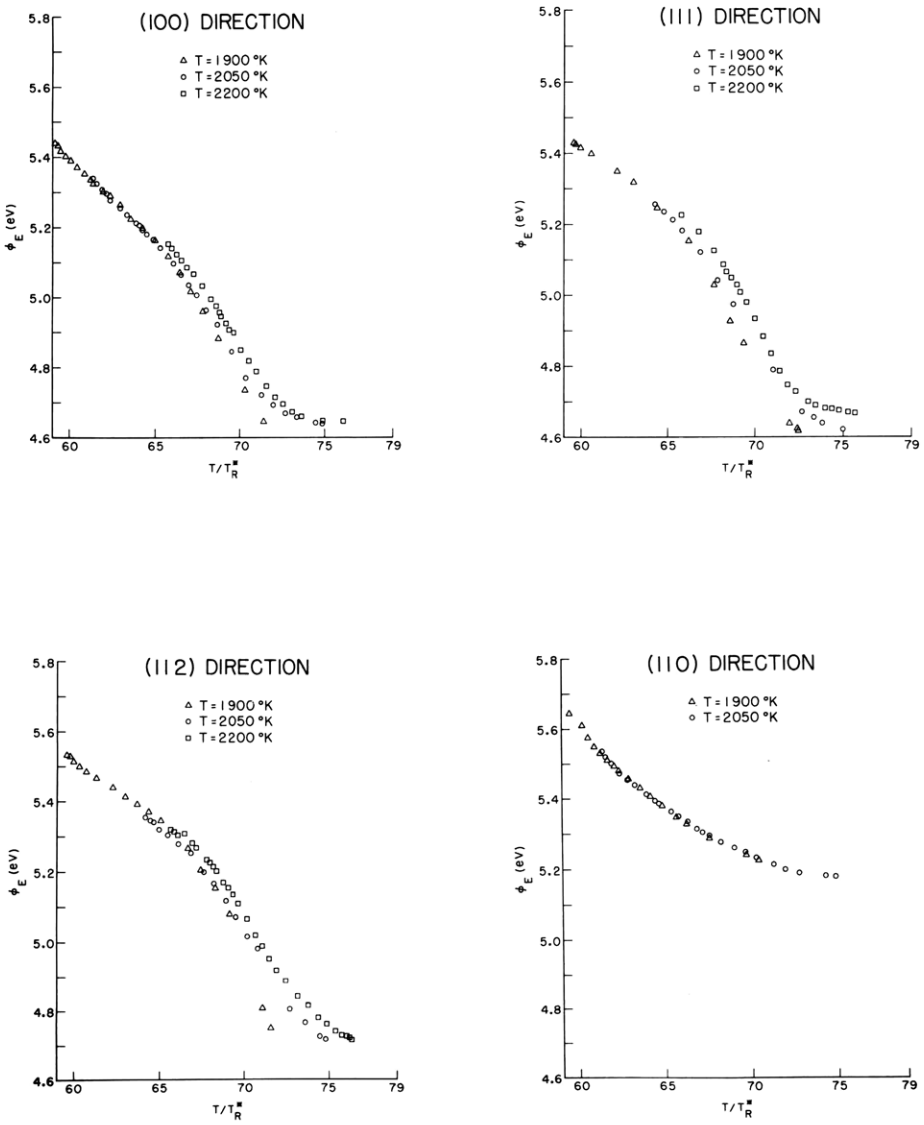

Fig. VIII-4. Effective function of the (100), (111), (112), and (110) crystallographic directions as a function of T/T_R^*.

$$I = 120\, ST^2 \exp\left(-\frac{\phi_E}{kT}\right), \tag{1}$$

where I is the measured collector current, S is the filament area subtended by the anode slit, k is Boltzmann's constant, and T is the filament temperature. We have not extrapolated the measurements of I to zero-field conditions because this correction has only a small effect on ϕ_E (~0.05 eV) for the anode voltage of 500 volts employed here.

The pressures reported in Fig. VIII-3 were measured with a General Electric ionization gauge (Model 22GT102). The thoria-coated iridium filament in the gauge was used to reduce the errors associated with interactions occurring at a hot filament. Since the sensitivity of ionization gauges is not well known for oxygen, we have chosen to express the pressure in terms of the equivalent nitrogen pressure. (The true O_2 pressure may differ from the equivalent N_2 pressure by as much as 25 per cent.)

The residual gas pressure increases with increasing filament temperature. This fact is illustrated in Fig. VIII-3; the minimum pressure shown for each filament temperature represents the pressure of the residual gases when the O_2 valve is closed. Hence the pressure readings are the sum of the O_2 pressure and the pressure of the unknown residual gases. Although this introduces an uncertainty in the low-pressure data, this effect becomes negligible at higher pressures.

Notice that the low-pressure limiting values of ϕ_E shown in Fig. VIII-3 are not the same for all filament temperatures. This result is to be expected if ϕ_E depends on temperature, if S is not measured accurately, or if the pre-exponential factor appearing in the Richardson equation is not 120 as assumed.

Since the O_2 coverage, θ, has not been measured in this experiment, we are unable to construct plots of ϕ_E versus θ. As an alternative, it is of interest to determine whether the parameter that is useful for correlating thermionic data for alkali metals[4] will also be successful for oxygen, The parameter is T/T_R, where T is the substrate (i.e., filament) temperature and T_R is the saturation temperature corresponding to the particular operating pressure of the gaseous adsorbate. The effective saturation temperatures, T_R^*, employed in Fig. VIII-4 are computed from the following empirical expression which accurately describes data reported by Honig and Hook[5] for the vapor pressure of oxygen:

$$\log_{10} p = 9.25 - \frac{486.45}{T_R^*}. \tag{2}$$

Since the reciprocal of T/T_R^* may be considered as a measure of the converage, it follows that ϕ_E should appraoch the clean-surface value as T/T_R^* increases.

The correlation shown in Fig. VIII-4 is surprisingly good. The scatter appearing at high values of T/T_R^* may be caused by the factors discussed previously in connection with the data of Fig. VIII-3. The comparison of the different crystallographic directions

shown in Fig. VIII-3 is based on curves drawn through the data points of Fig. VIII-4.

Discussion of Results

The effect of O_2 on the thermionic emission from W was first studied by Kingdon, in 1924.[6] A similar investigation was performed in greater detail by Johnson and Vick, in 1937.[7] Polycrystalline tungsten filaments were employed in both experiments, and the O_2 pressure was not accurately measured.

Using the contact-potential method, Langmuir and Kingdon[8] measured work-function changes for O_2 on W which were much smaller than those computed from the thermionic data of Kingdon.[6] Reimann[9] repeated the contact-potential measurements and obtained a maximum contact-potential change of 1.7 eV for O_2 on W at room temperature. This value is in good agreement with that computed from Kingdon's data, and it has been verified in subsequent investigations both with the field-emission microscope and the contact-potential method.[10] A detailed study of the change in contact potential with increasing O_2 coverage on polycrystalline W has been performed by Bosworth and Rideal.[11]

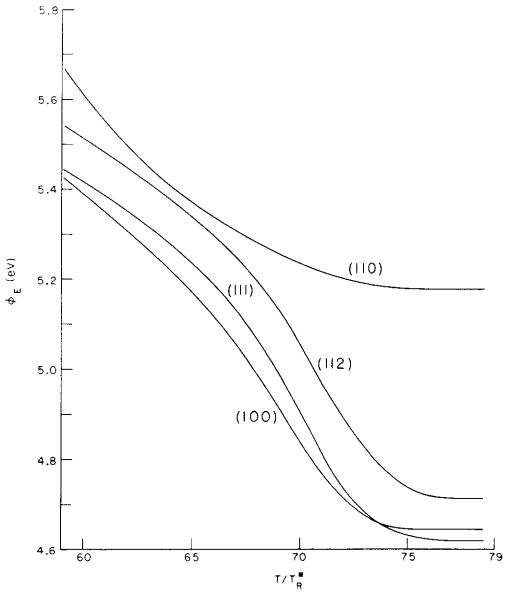

Fig. VIII-5.
Comparison of the average experimental results for O_2 on W; ϕ_E vs T/T_R^* for the (100), (111), (112), and (110) crystallographic directions.

Since the results of the present study are, to the best of our knowledge, the first thermionic measurements of the effect of O_2 on the work function of a single-crystal substrate, we have no standard comparison. Becker and Brandes[12] have, however, used the field-emission microscope to investigate the effect of O_2 on various crystallographic planes of W. The general characteristics of our results agree qualitatively with those of Becker and Brandes. Quantitative agreement is not expected, because of the significant differences in the experimental techniques. Mueller,[13] Gomer and Hulm,[14] and George and Stier[15] have also used the field-emission microscope to study O_2 on W.

As seen in Fig. VIII-5, the maximum work-function change determined from the present data is ~0.83 eV. This value is less than that measured in contact-potential studies because the filament temperature is sufficiently high to reduce the O_2 coverage below the maximum possible value. As inferred in the selection of T/T_R^* as the

correlation parameter, the coverage increases with increasing pressure and decreasing filament temperature. It is expected that, for the range of pressures and temperatures used here, the surface coverage does not exceed one monolayer of atomic oxygen.[12, 16]

Although the structure of O_2 on W is not completely understood, there is evidence that absorption and surface rearrangement is greatest on crystallographic planes having an open-lattice structure.[17] This provides a possible explanation for the fact that the work function of the (110) direction is not affected by O_2 as markedly as the other crystallographic directions (Fig. VIII-5). (We prefer to use the term "crystallographic direction" instead of "crystallographic plane" because the exact surface structure of the tungsten filament is not known.)

W. Engelmaier, R. E. Stickney

References

1. I. Langmuir and K. H. Kingdon, Phys. Rev. 23, 112 (1923).
2. J. M. Houston and H. F. Webster, in Advances in Electronics and Electron Physics, Vol. 16, L. Marton (ed.) (Academic Press, New York, 1962), p. 167.
3. For example, see R. L. Aamodt, L. J. Brown, and B. D. Nichols, J. Appl. Phys. 33, 2080 (1962); L. S. Swanson, R. W. Strayer, and F. M. Charbonnier, Report on Twenty-fourth Annual Conference on Physical Electronics, p. 120, 1964, C. H. Skeen, J. Appl. Phys. 36, 84 (1965); also see the Reports on the 1964 and 1965 Thermionic Conversion Specialist Conferences.
4. N. S. Rasor and C. Warner, J. Appl. Phys. 35, 2589 (1964); For a thermionic treatment, see E. N. Carabateas, J. Appl. Phys. 33, 2698 (1962).
5. R. E. Honig and H. O. Hook, R. C. A. Review 21, 360 (1960).
6. K. H. Kingdon, Phys. Rev. 24, 510 (1924).
7. M. C. Johnson and F. A. Vick, Proc. Roy. Soc. (London) A151, 308 (1935).
8. I. Langmuir and K. H. Kingdon, Phys. Rev. 34, 129 (1929).
9. A. L. Reimann, Phil. Mag. 20, 594 (1935).
10. The results of these investigations have been summarized by R. V. Culver and F. C. Tompkins, Advances in Catalysis 11, 67 (1959) (Academic Press, New York).
11. R. C. L. Bosworth and E. K. Rideal, Physica 4, 925 (1937); also see R. C. L. Bosworth, Proc. Roy. Soc. (New South Wales) 79, 190 (1946).
12. J. A. Becker and R. G. Brandes, J. Chem. Phys. 23, 1323 (1955).
13. E. W. Mueller, Ergeb. exakt. Naturw. 29, 290 (1953).
14. R. Gomer and J. K. Hulm, J. Chem. Phys. 27, 1363 (1957).
15. T. H. George and P. M. Stier, J. Chem. Phys. 37, 1935 (1962).
16. J. A. Becker, E. J. Becker, and R. G. Brandes, J. Appl. Phys. 32, 411 (1961).
17. J. A. Becker, Advances in Catalysis 7, 135 (1955); R. Gomer, Advances in Catalysis 7, 93 (1955); N. J. Taylor, Surface Science 2, 544 (1964); J. Anderson and W. E. Danforth, J. Franklin Inst. 279, 160 (1965).

2. CONTACT POTENTIAL MEASUREMENTS OF THE WORK FUNCTION OF TANTALUM AS A FUNCTION OF CESIUM COVERAGE

Introduction

The primary objective of this report is to describe an experimental apparatus designed to determine the dependence of the work function of a well-defined metallic substrate on alkali-metal coverage. As an illustration of the experimental technique to be used, preliminary results obtained for cesium upon a polycrystalline tantalum substrate are presented. In subsequent studies a single-crystal substrate will be employed to satisfy the condition of a reasonably well-defined, uniform surface.

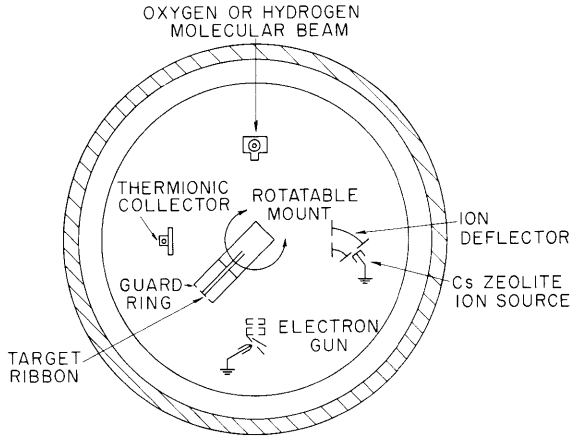

Fig. VIII-6. Schematic diagram of the apparatus.

Apparatus

As a prerequisite for any precise surface adsorption study, it is imperative that the surface of interest be kept free of contamination from background gases. Here, this condition is met by mounting the apparatus, shown schematically in Fig. VIII-6, within a Varian ultrahigh vacuum system. The stainless-steel chamber, with a working space of 45×90 cm, is evacuated by a 500 l/s ion pump. For additional pumping in the ultra-high vacuum region, titanium is sublimated upon liquid-nitrogen cold panel. Since this system can achieve pressures in the low 10^{-10} Torr range ($\sim 3 \times 10^{-10}$ Torr for these runs), it is possible to maintain contamination-free surface conditions for times much longer than those required for an experimental run.

The apparatus has been designed to furnish information in the most meaningful way to enable us to carry out our primary objective. The specimen to be studied is a tantalum ribbon, $0.0025 \times 0.127 \times 2.54$ cm, mounted on a rotatable shaft. (The preliminary runs utilized a polycrystalline specimen; in subsequent runs a (110) monocrystal will be studied.) Cleaning of the surface is achieved by direct resistive heating to ~2500°K.

Alkali-metal deposition upon the target is obtained by using a zeolite ion source containing the desired alkali.[1] Since the target temperature is maintained at 300°K during a run, this method allows us to attain and maintain alkali-metal coverages without flooding the entire system with alkali vapor. Also, by monitoring the collected ion current, the number of alkali-metal ions deposited can be directly and accurately known. The source is a thin layer of alkali-metal zeolite fused to a platinum ribbon $0.005 \times 0.635 \times 5.1$ cm. This ribbon, heated by direct resistive heating,

is run at 800-900°C to obtain sufficient ion emission (10^{-7}-10^{-6} amps/cm^2 for the preliminary Cs runs). The emitted ions are accelerated through a 0.635 × 2.54 cm slit, electrostatically deflected in a 60° analyzer, and beamed on the target through another 0.635 × 2.54 cm slit. The electrostatic analyzer decreases the possiblity of neutral contamination from the source. For the preliminary runs, the maximum potential applied between the target and the source is 8 volts.

Changes of substrate work function because of alkali-metal adsorption are measured by the contact-potential method.[2,3] For this measurement, the target is positioned before a simple electron gun of the Farnsworth style.[4] This gun has a polycrystalline tantalum filament mounted off-center to prevent photoelectric effects and direct contamination. Since the method requires constant emitter conditions, the filament is continually run at ~2100°K, and its center is grounded.

Used alone, the contact-potential method tells nothing about absolute work functions. If, however, the bare-surface work function is known subsequent contact-potential measurements can be converted to absolute values. In this apparatus, the thermionic work function of the clean target is measured by positioning the target at the therionic measurement station. This station consists of a collector, subtending a center portion of the tantalum ribbon, bounded by two guard rings. The geometry of this station is planar.

As shown in Fig. VIII-6, the target may also be positioned before an oxygen/hydrogen molecular beam. Diffusion leaks are used to supply the oxygen or hydrogen required to form the beam. Such a beam serves a double purpose. First, oxygen is useful in the cleaning of the surface.[5] Second, the molecular beam allows us to study the effect of additive gases on the work function of alkali-metal covered surfaces. Such studies, though interesting in their own right, serve as important standards against which the uncontaminated data may be checked.

As well as controlled contamination runs, quantitative studies will be made with the use of a G. E. monopole partial pressure analyzer. These studies will quantitatively check adsorbate purity and unwanted background contamination. The device is available and can easily be attached to the system.

A liquid-nitrogen cold finger may be added for two auxiliary studies. Cooling the surface will allow studies at high overlayer coverages and provide a check on the possible dependence of work function upon temperature.

Experimental Method

Changes in the target work function are measured by the contact-potential method. The principles of this method are schematically shown in Fig. VIII-7. The potential energy diagram for an emitter with a constant work function, ϕ_E, and a collector with a clean function, ϕ_o, is shown in drawing A. In the case shown, a voltage, $V_o = \phi_E - \phi_o$,

is applied to the collector. This voltage is the contact potential difference between the emitter and the clean collector. Drawing A corresponds to the break point in the solid curve ℓn vs V; for collector voltages greater than V_o, the electrons are retarded and the Boltzmann portion of the curve is obtained. If the work function of the collector is

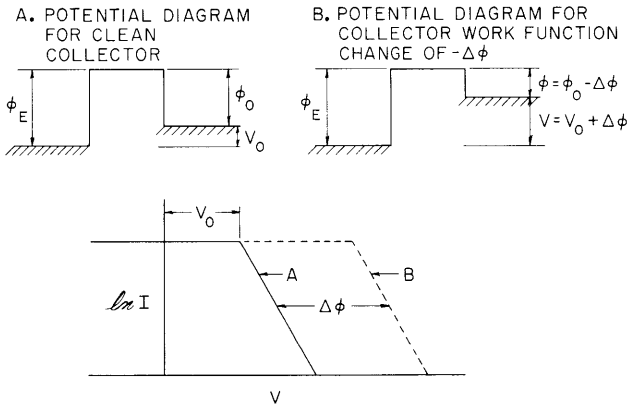

Fig. VIII-7. Illustrating the contact-potential method.

decreased, the situation is that shown in drawing B. Here again the voltage applied, $V = \phi_E - \phi_o + \Delta\phi$, is the contact potential. Thus, changing the work function of the collector (relative to the emitter) by $\Delta\phi$ changes the contact potential by $\Delta\phi$. The net result is that the Boltzmann portion of the I-V plot is shifted, parallel to the clean plot, by an amount $\Delta\phi$. Thus, to measure changes in the collector work function, we need measure only the shift of the I-V plot relative to the clean plot.

The contact potential method has two primary advantages: it measures changes of work function directly; and since the collector is kept at ~300°K, alkali-metal coverage

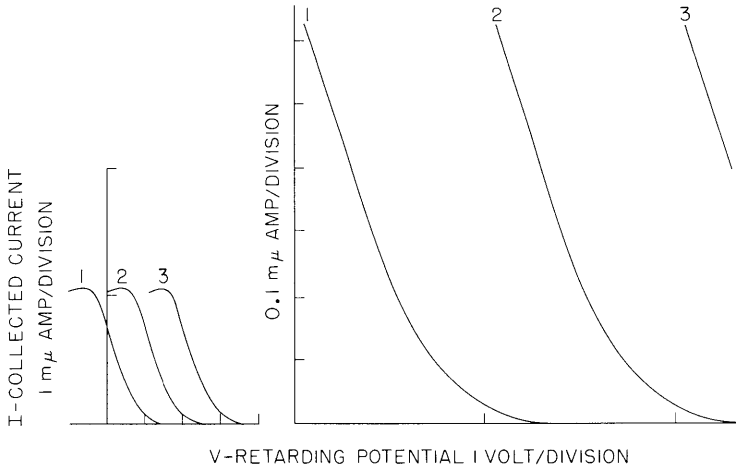

Fig. VIII-8. Typical retarding-potential plots.

can be maintained without a high background pressure of alkali-metal vapor. The main disadvantage is that the method measures only changes and not absolute values; however, this is overcome by making an independent measurement of the thermionic work function of the surface. (The work function characterizing the emission of electrons at high temperatures will equal that characterizing the collection of electrons at room temperatures only if the properties of the surface are uniform and independent of temperature.)

The actual experimental method is best understood by referring to Fig. VIII-8. For each run, two retarding-potential plots are made. The small-scale plots, at the left in Fig. VIII-8, allow qualitative comparisons of different runs while the expanded-scale plots allow quantitative comparisons of the highly retarded portions of different runs. For instance, curve 1 represents a retarding-potential plot for a cleaned surface. Subsequent plots with adsorbed alkali-metal films (e.g., curves 2 and 3) are considered satisfactory for quantitative comparisons only if they are parallel to the clean curve (within ~0.03 eV) and show the same saturation current. In order for such standards to be valid, however, background contamination must be negligible.

The possibility of background contamination is checked in the following way. After each run with an adsorbed alkali-metal film, the surface is flashed and a retarding-potential plot is taken. To ensure reproducibility of the clean surface, this plot must always coincide with curve 1. An occasional contamination check is then made by allowing the clean surface to sit for a time (~20 minutes) longer than the maximum time for a run (~9 minutes). If, during this time, the surface contaminates enough to shift the curve by greater than ~0.02 eV, the previous runs are discarded.

Results for Cesium on Tantalum

The experimental results for cesium upon polycrystalline tantalum are shown in Fig. VIII-9 where work function change is plotted against the number of cesium ions applied. Three features of this plot are worth noting. First, at low coverage the work function decreases almost linearly with coverage. Second, the curve shows a maximum work function decrease (~2.47 eV at a coverage of 7×10^{13}). Third, though more high-coverage data are needed, the work-function change at high coverages appears to reach a limiting value (~2.21 eV).

To compare the data eventually with theoretical predictions, we must convert the number of cesium applied into a fractional coverage, θ. For convenience we have assumed one-monolayer coverage ($\theta = 1$) to be the point where the curve of Fig. VIII-9 becomes flat. Quantitatively, $\theta = 1$ is defined as the point where 15.5×10^{13} cesium paricles have been applied to the surface. By this definition, the curve is linear up to approximately $\theta = 0.15$, and the minimum occurs at approximately $\theta = 0.5$. It is also interesting to note that if we divide the number of cesium in a monolayer (15.5×10^{13}) by the apparent target area exposed to the cesium beam (~0.322 cm^2), the monolayer

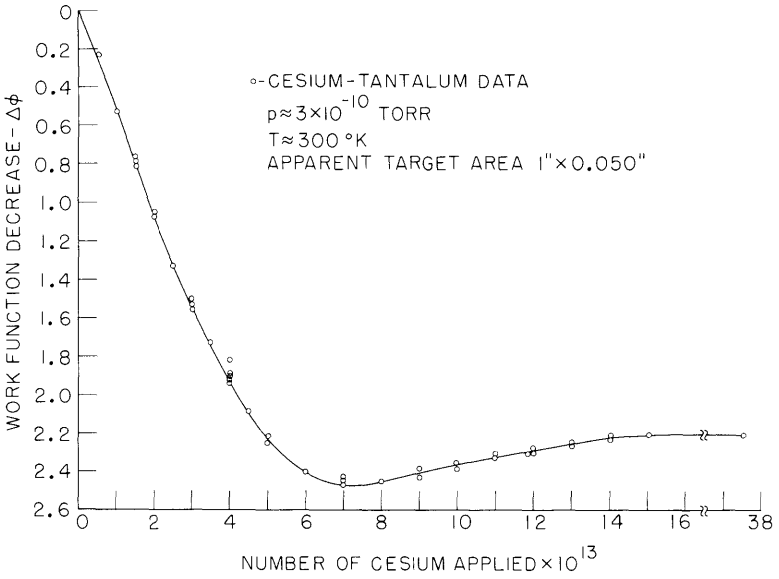

Fig. VIII-9. Experimental data for Cesium on Tantalum.

denisty of cesium is found to be $\sigma = 4.8 \times 10^{14}$ cesium/cm^2. This is the same value Taylor and Langmuir used for cesium upon a rough tungsten surface.[6]

Faulty design of the present thermionic measuring station made it difficult to obtain a reliable measurement of the work function of the bare tantalum surface. Despite this, a thermionic bare-surface work function of 4.15 + 0.1 eV was estimated from the thermionic measurements. Based on this value, the minimum work function occurring near $\theta = 0.5$ is found to be 1.68 ± 0.1 eV, and the limiting value for full coverage is 1.94 ± 0.1 eV.

It must be recognized that these numbers are only approximations. For a patchy surface, a thermionic measurement will accentuate low work-function patches, while the contact-potential method attaches more relevance to an averaged work function.[3] Using the thermionically measured work function for the 300°K surface is also dubious if the work function displays a strong dependence upon temperature.

Beyond these two points there is another serious point to be raised. If appreciable cesium atom desorption occurs at high coverages, serious doubt is cast upon our definitions of coverage. Since we have no way of measuring atomic desorption rates, two limiting cases have been calculated by using an expression derived by Rasor and Warner.[7] If, as Rasor and Warner assume, the atomic heat of adsorption is constant at all coverages and has a value of ~1.6 eV for cesium upon tantalum, no appreciable desorption will occur until coverages near $\theta = 0.99$ are reached. If, on the other hand, the heat of adsorption at high coverage tends toward the value for vaporization of bulk cesium (~0.80 eV) serious desorption would begin at coverages of $\theta \approx 0.7$. The fact

that the data give a reasonable value for monolayer density (σ) may indicate that the former case is the more likely.

Comparison with Existing Experimental Data

Houston[8] has reported some emission data for cesium on polycrystalline tantalum. Since Houston did not measure coverage and it is difficult to compare thermionic data with contact potential data, only a qualitative comparison will be made. Most important, the data of Houston indicate the existence of a minimum work function and, for a bare work function of ~4.3 eV, the minimum value found is ~1.6 eV. Since our bare work function is ~4.15 eV, our minimum value of 1.68 eV is only in qualitative agreement with Houston's value.

D. L. Fehrs, R. E. Stickney

References

1. R. E. Weber and L. F. Cordes, Report on the Twenty-fifth Annual Conference on Physical Electronics, M.I.T., 1965, p. 378.
2. P. A. Anderson, Phys. Rev. 47, 958 (1935).
3. W. B. Nottingham, Thermionic Emission, Technical Report 321, Research Laboratory of Electronics, M.I.T., December 10, 1956, p. 110.
4. H. E. Farnsworth, Rev. Sci. Instr. 21, 102 (1950).
5. J. A. Becker, E. J. Becker, and R. G. Brandes, J. Appl. Phys. 32, 411 (1961).
6. J. B. Taylor and I. Langmuir, Phys. Rev. 44, 433 (1933).
7. N. S. Rasor and C. Warner, III, J. Appl. Phys. 35, 2589 (1964).
8. J. M. Houston and P. K. Dedrick, Report on the Thermionic Conversion Specialist Conference, Cleveland, Ohio, 1964, p. 77.

VIII. PHYSICAL ELECTRONICS AND SURFACE PHYSICS

C. Free-Molecule Flow Fields*

Academic and Research Staff

Prof. R. E. Stickney

Graduate Students

Y. S. Lou
S. Yamamoto

1. INVESTIGATION OF FREE-MOLECULE FLOW FIELDS

The general objective of this research project is to study the fluid dynamics of the transition regime existing between the free-molecule and continuum limits. Rather than using wind-tunnel techniques to study the transition flow around bodies, we have chosen to study the flow through orifices and tubes for the following reasons: (i) the orifice geometry is particulary well suited, since it minimizes the effect of unknown gas-surface interactions on the flow;[1] (ii) theoretical solutions are known, at least in principle, for the limiting cases of free-molecule and continuum flow through orifices and tubes;[1-3] (iii) the geometry of the apparatus permits us to measure the velocity distribution of the flow, thereby providing information that is more detailed than that generally available in wind tunnel tests; (iv) the cost and size of the apparatus are more reasonable; and (v) the experimental results will be relevant to engineering problems of molecular beam generation, exhaust of gases into space, and the flow of gases in vacuum systems.

We have recently completed an experimental investigation of the angular distribution of flow from orifices and tubes in the near-free molecule regime.[4] Although these results provide useful information on the nature of the flow, measurements of the velocity distribution are now desirable because such data provide a complete description which could be used to check and to improve the existing theoretical treatments.

Although the velocity distributions of molecular beams have been studied by a number of investigators,[5-12] the results are incomplete because the experiments were limited to a small range of Knudsen numbers; the designs were such that measurements were restricted to one direction, that of the center line of the flow; and, in many cases, the experiments employed tubes or slits instead of sharp-edged orifices. (Since most theoretical treatments consider orifice flow,[13-15] it is most important to obtain data for this type of aperture.) We believe that it is possible to circumvent all of these limitations by using the technique described below. Also, this technique enables us to

*This work was supported by the National Aeronautics and Space Administration (Grant NsG-496).

make absolute measurements for cesium because all of the molecules striking the detector are ionized and recorded.

Since the basic features of the experimental apparatus have been described in previous progress reports, we shall concentrate here on the modifications that were required for measurements of the velocity distribution. The technique is similar to the time-of-flight method employed by Knauer[11] and Kofsky.[12] The molecular beam is interrupted periodically by a rotating disc driven by an electric motor, thereby creating pulses of molecules. The time, Δt, required for molecules in a given pulse to reach the detector is simply related to their speed, v, and the distance from the rotating disc to the detector, ℓ,

$$\Delta t = \frac{\ell}{v}.$$

Hence, the faster molecules will arrive at the detector before the slower ones. By displaying the detector signal on an oscilloscope, we obtain a waveform that may be related to the velocity distribution function. (A Moseley Waveform Translator (Type 101) may be used together with an X-Y recorder to obtain a permanent, enlarged record of the waveform.)

Some preliminary results are shown in Figs. VIII-10 and VIII-11. The solid curves represent the theoretical waveforms which would result if the flow were completely free molecular; the experimental data points are taken from waveform measurements. We would expect experiment to agree with theory when the Knudsen number (defined here as the ratio of the mean-free path, λ, to the orifice diameter, D) is sufficiently greater than unity. Hence, the agreement obtained for $\lambda/D = 10.2$ (Fig. VIII-10) is an indication that our apparatus is functioning properly.

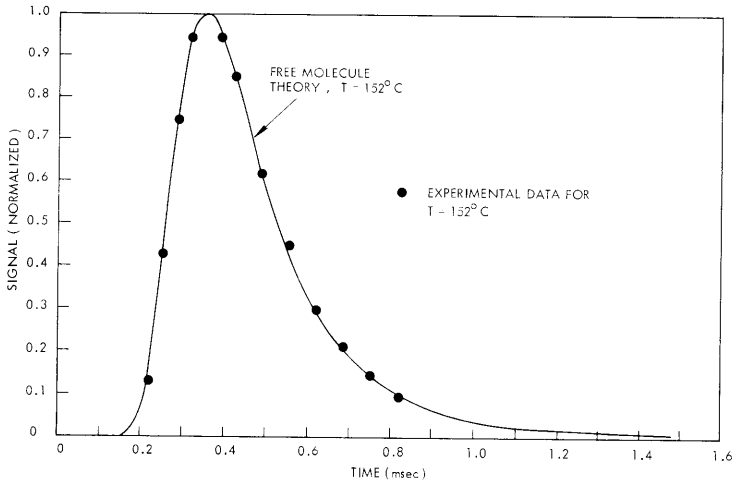

Fig. VIII-10. Experimental results for T = 152°C.

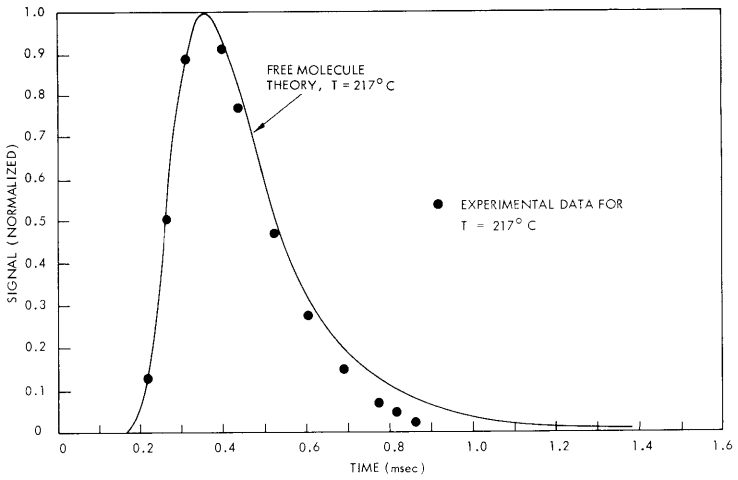

Fig. VIII-11. Experimental results for T = 217°C.

According to the experimental[6-11] and theoretical results reported by others, the normalized velocity distribution for flow from an orifice should exhibit a deficiency of low-speed molecules when λ/D is of the order of unity. A deficiency of this nature is observed in Fig, VIII-11 for $\lambda/D = 0.85$. (As stated previously, the molecular speed is inversely proportional to time.)

At the present time we are obtaining data over a range of Knudsen numbers and for various angles from the flow center line. Tubes having different length-to-diameter ratios will be investigated after completing the orifice experiments.

R. E. Stickney, Y. S. Lou, S. Yamamoto

References

1. H. W. Liepmann, J. Fluid Mech. 10, 65 (1961).
2. W. G. Pollard and R. D. Present, Phys. Rev. 73, 762 (1948).
3. S. Dushman and J. M. Lafferty, Scientific Foundations of Vacuum Technique (John Wiley and Sons, Inc., New York, 1962).
4. See pages 19-21 of the Fifth Semiannual Progress Report, M. I. T. Center for Space Research, December 1965.
5. A review of the early measurements of velocity distribution is presented in E. H. Kennard, Kinetic Theory of Gases (McGraw-Hill Book Company, New York, 1938).
6. A. Ellett and V. W. Cohen, Phys. Rev. 52, 509 (1937).
7. I. Estermann, O. C. Simpson, and O. Stern, Phys. Rev. 71, 238 (1947).
8. A. Bennett, Phys. Rev. 95, 608 (1954).
9. P. M. Marcus and J. H. McFee, in Recent Research in Molecular Beams, I. Estermann (ed.) (Academic Press, Inc., New York, 1959), p. 43.
10. J. E. Scott, H. S. Morton, J. A. Phipps, and J. F. Moonan, Proc. 4th International Symposium on Rarefied Gas Dynamics, 1964 (to be published).

11. F. Knauer, Z. Physik 126, 319 (1949).

12. I. L. Kofsky, S. M. Thesis, Physics Department., Syracuse University, 1948.

13. R. Narasimha, J. Fluid Mech. 10, 381 (1961).

14. D. R. Willis, J. Fluid Mech. 21, 21 (1965).

15. H. S. Morton, Project Squid Technical Report UVA-4-P-1, University of Virginia, 1948.